SCIENCE AND TECHNOLOGY ORGANIZATION
CENTRE FOR MARITIME RESEARCH AND EXPERIMENTATION

Reprint Series **CMRE-PR-2014-004**

Ray convergence in a flux-like propagation formulation

Chris H. Harrison

January 2014

Originally published in:

Journal of the Acoustical Society of America, Vol. 133 (6), 2013, pp. 3777-3789.

About CMRE

The Centre for Maritime Research and Experimentation (CMRE) is a world-class NATO scientific research and experimentation facility located in La Spezia, Italy.

The CMRE was established by the North Atlantic Council on 1 July 2012 as part of the NATO Science & Technology Organization. The CMRE and its predecessors have served NATO for over 50 years as the SACLANT Anti-Submarine Warfare Centre, SACLANT Undersea Research Centre, NATO Undersea Research Centre (NURC) and now as part of the Science & Technology Organization.

CMRE conducts state-of-the-art scientific research and experimentation ranging from concept development to prototype demonstration in an operational environment and has produced leaders in ocean science, modelling and simulation, acoustics and other disciplines, as well as producing critical results and understanding that have been built into the operational concepts of NATO and the nations.

CMRE conducts hands-on scientific and engineering research for the direct benefit of its NATO Customers. It operates two research vessels that enable science and technology solutions to be explored and exploited at sea. The largest of these vessels, the NRV Alliance, is a global class vessel that is acoustically extremely quiet.

CMRE is a leading example of enabling nations to work more effectively and efficiently together by prioritizing national needs, focusing on research and technology challenges, both in and out of the maritime environment, through the collective Power of its world-class scientists, engineers, and specialized laboratories in collaboration with the many partners in and out of the scientific domain.

NOTE: The CMRE Reprint series reprints papers and articles published by CMRE authors in the open literature as an effort to widely disseminate CMRE products. Users are encouraged to cite the original article where possible.

Ray convergence in a flux-like propagation formulation

Chris H. Harrison[a)]
Centre for Maritime Research and Experimentation, Viale San Bartolomeo 400, 19126 La Spezia, Italy

(Received 16 November 2012; revised 20 March 2013; accepted 25 March 2013)

The energy flux formulation of waveguide propagation is closely related to the incoherent mode sum, and its simplicity has led to development of efficient computational algorithms for reverberation and target echo strength, but it lacks the effects of convergence or modal interference. By starting with the coherent mode sum and rejecting the most rapid interference but retaining beats on a scale of a ray cycle distance it is shown that convergence can be included in a hybrid formulation requiring minimal extra computation. Three solutions are offered by evaluating the modal intensity cross terms using Taylor expansions. In the most efficient approach the double summation of the cross terms is reduced to a single numerical sum by solving the other summation analytically. The other two solutions are a local range average and a local depth average. Favorable comparisons are made between these three solutions and the wave model Orca with, and without, spatial averaging in an upward refracting duct. As a by-product, it is shown that the running range average is very close to the mode solution excluding its fringes, given a relation between averaging window size and effective number of modes which, in turn, is related to the waveguide invariant.
 [http://dx.doi.org/10.1121/1.4802642]

PACS number(s): 43.30.Bp, 43.30.Cq, 43.30.Es [JAI]

I. INTRODUCTION

The flux approach to calculating propagation loss (Weston, 1959, 1960, 1980a,b,c) and the incoherent mode sum (Brekhovskikh and Lysanov, 2003, p. 129) can be shown to be closely related (see, e.g., Harrison and Ainslie, 2010), and both predict a monotonic decay with range of the form $r^{-1}\sum_n \exp(-a_n r)$, i.e., "mode stripping." This approach has been successfully applied to find closed-form reverberation assuming isovelocity water (Zhou, 1980) and for both target echo and reverberation assuming isovelocity and variable bathymetry (Harrison, 2003), bistatic geometry (Harrison, 2005b) and limited refraction (Harrison, 2005a). The sonar performance model Artemis (Harrison, 2011a) handles variable bathymetry and sound speed in a general way but still based on an incoherent mode sum. However, if the sound speed profile causes significant refraction this otherwise good approximation may be spoilt by convergence, focusing, and caustics. These effects are familiar in deep water as "convergence zones" (Urick, 1967, pp. 151–152; Tolstoy and Clay, 1987, p. 145–150; Beilis, 1983; Baggeroer, *et al.*, 2010) and also in shallow water as patterns of caustics that are strongly dependent on source depth (Brekhovskikh and Lysanov, 2003, p. 121). It is straightforward to predict these effects using wave models such as CSNAP (Ferla *et al.*, 1993), RAM (Collins, 1993), or ORCA (Westwood *et al.*, 1996), but the benefit of this incoherent mode approach is computational speed. The objective of this paper is to extend these methods to include convergence effects without compromising computation time. Fundamentally, this will be done by retaining part, but not all, of the interference field (i.e., coherence) while adopting a formula that requires only very slight increase in computation time over the incoherent calculation. In this context, the approach rejects terms that result in interference on a scale close to an acoustic wavelength and instead concentrates on interference on a scale of a ray cycle distance, namely, interference between adjacent modes. This contrasts with some earlier work where a similar starting point provided insight into the waveguide invariant (Harrison, 2011b) and multipath group velocities (Harrison, 2012a).

Note that convergence effects are most significant for refracting paths, whether refracted in the water column or seabed sediments. In practice, with simple bottom reflection properties, convergence is important for paths whose turning point velocities are within the range of the water column sound speeds. In contrast the steeper paths reflecting from both boundaries tend not to converge since they are relatively straight. Nevertheless even in isovelocity water localized peaks in depth are still possible (see Weston, 1980c).

In this paper propagation is calculated as a function of range and depth with launch angle as a parameter. Since angle is related to travel time, convergence can alternatively be viewed as a function of time. The impulse response of a point target, say, tends to have all the convergence effects concentrated near the first return with late arrivals tending to decay more or less monotonically with time (Harrison and Nielsen, 2007). For the same reason reverberation may consist of a mixture of monotonic decaying and convergent paths. Long range reverberation requires propagation paths to interact with at least one boundary, possibly disallowing a large proportion of the angle range with potential for convergence. Nevertheless significant convergence effects are still possible with reverberation.

[a)]Author to whom correspondence should be addressed. Also at: Institute of Sound and Vibration Research, University of Southampton, Highfield, Southampton SO17 1BJ, United Kingdom. Electronic mail: harrison@cmre.nato.int

Although the results will be seen to be closely related to ray solutions some of the difficulties associated with ray accounting are avoided by basing everything firmly on a normal mode approach. Despite the links between rays and modes being well known (Brekhovskikh and Lysanov, 2003, p. 140–143; DiNapoli and Deavenport, 1979, p. 117–121) this approach shows the connection between a running range average, a local depth average, and very coarse modal interference fringes, all of which have potential for providing a convergence correction to cylindrical spreading.

For clarity in the following development modal attenuation is omitted. However, it is straightforward to include modal decay because the derivations below rely on analytical summation of oscillatory terms which are only weakly influenced by attenuation. The solutions are explicitly integrals over angle (at the source), and for each angle the losses accumulate additively in range.

II. DERIVATIONS

A. Sum of modes in terms of ray cycles

The ratio of the pressure-squared at r, z_r to the pressure-squared at unit distance from a source at 0, z_s can be written as the modulus square of the coherent sum of M modes $\phi_m(z)$ in water of uniform density (Brekhovskikh and Lysanov, 2003, p. 129)

$$\begin{aligned} P &= 2\pi\left|\sum_{m=1}^{M}\frac{\phi_m(z_s)\,\phi_m(z_r)}{\sqrt{K_m r}}\exp(iK_m r)\right|^2 \\ &= 2\pi\sum_{n=1}^{M}\frac{{\phi_n}^2(z_s)\,{\phi_n}^2(z_r)}{K_n r} \\ &\quad + 2\pi\sum_{n=1}^{M}\sum_{m=1}^{n-1}\frac{\phi_n(z_s)\,\phi_n(z_r)\,\phi_m(z_s)\,\phi_m(z_r)}{\sqrt{K_n K_m}\,r} \\ &\quad \times 2\cos[(K_n-K_m)r] \equiv P_1 + P_2. \end{aligned} \tag{1}$$

Note that the first term, P_1, is the incoherent mode sum, and the second, P_2, consists of all the cross terms. Adopting Wentzel–Kramers–Brillouin (WKB) modes with normalization A_n as in Appendix A, writing the vertical wave number γ_n in terms of the depth-dependent wave number $k(z)$ and the eigenvalue (horizontal wave number) K_n as

$$\gamma_n(z) = \sqrt{k^2(z) - {K_n}^2} \tag{2}$$

and using the shorthand for its integral (from the bottom ray turning point z_B to z_o)

$$w_n(z_o) = \int_{z_B}^{z_o}\sqrt{k^2(z) - {K_n}^2}\,dz - \varepsilon_B \tag{3}$$

(ε_B is a small integration constant that has no effect on the results, as will be seen),

$$P_1 = 2\pi\sum_n \frac{{A_n}^4\sin^2[w_n(z_s)]\sin^2[w_n(z_r)]}{\gamma_n(z_s)\gamma_n(z_r)K_n r}. \tag{4}$$

Excluding the case where $z_r = z_s$ exactly (see Weston, 1980c) the local mean is

$$P_1 = 2\pi\frac{{A_n}^4}{4}\sum_n \frac{1}{\gamma_n(z_s)\gamma_n(z_r)K_n r}. \tag{5}$$

The second term on inserting WKB modes becomes

$$\begin{aligned} P_2 = 2\pi\sum_{n=1}^{M}\sum_{m=1}^{n-1}&{A_n}^2{A_m}^2 2\cos[(K_n-K_m)r] \\ &\times \frac{\sin[w_n(z_s)]\sin[w_m(z_s)]\sin[w_n(z_r)]\sin[w_m(z_r)]}{\sqrt{\gamma_n(z_s)\,\gamma_n(z_r)\,\gamma_m(z_s)\,\gamma_m(z_r)}\sqrt{K_n K_m}\,r}. \end{aligned} \tag{6}$$

Now the product of each pair of sines can be written in terms of cosines of sum and difference:

$$\begin{aligned} S &= 2\sin[w_n(z_{s,r})]\sin[w_m(z_{s,r})] \\ &= \cos[w_n(z_{s,r}) - w_m(z_{s,r})] - \cos[w_n(z_{s,r}) + w_m(z_{s,r})]. \end{aligned} \tag{7}$$

If the rapidly oscillating second cosine term is rejected, then P_2 can be represented as the product of three cosines of differences

$$P_2 = 2\pi\sum_{n=1}^{M}\sum_{m=1}^{n-1}\frac{{A_n}^2{A_m}^2}{2}\frac{\cos[(K_n-K_m)r]\cos[w_n(z_s) - w_m(z_s)]\cos[w_n(z_r) - w_m(z_r)]}{\sqrt{\gamma_n(z_s)\,\gamma_n(z_r)\,\gamma_m(z_s)\,\gamma_m(z_r)}\sqrt{K_n K_m}\,r}. \tag{8}$$

Furthermore, it is easy to show that for arbitrary a, b, c,

$$\cos a \times \cos b \times \cos c = \frac{1}{4}\{\cos(a-b-c) + \cos(a-b+c) + \cos(a+b-c) + \cos(a+b+c)\}. \tag{9}$$

The following shorthand can be used to cover all four terms

$$\cos a \times \cos b \times \cos c = \frac{1}{4}\sum_4 \cos(a \pm b \pm c), \tag{10}$$

with $a \equiv (K_n - K_m)r$; $b \equiv w_n(z_s) - w_m(z_s)$; $c \equiv w_n(z_r) - w_m(z_r)$, so

$$P_2 = 2\pi \sum_{n=1}^{M} \sum_{m=1}^{n-1} \frac{{A_n}^2 {A_m}^2}{8} \frac{\sum_4 \cos\{[(K_n - K_m)r] \pm [w_n(z_s) - w_m(z_s)] \pm [w_n(z_r) - w_m(z_r)]\}}{\sqrt{\gamma_n(z_s)\,\gamma_n(z_r)\,\gamma_m(z_s)\,\gamma_m(z_r)}\sqrt{K_n K_m}\,r}. \tag{11}$$

Assuming that the most important effects come from modes that are not too far apart, i.e., for which $n - m = j$ is small, these differences can all be Taylor expanded and expressed in terms of the complete and partial ray cycle distances r_c, r_s, r_r (see Appendix B). (The partial cycle distances r_s, r_r are measured from one side of the duct to the source or receiver depth, respectively.) These are each related to the ray turning point velocity and the modal eigenvalue K_n. Higher order Taylor expansions will be investigated in Sec. III D and Appendix B, but to first order P_2 becomes

$$P_2 = 2\pi \sum_j \sum_n \frac{{A_n}^4}{8} \frac{1}{\gamma_n(z_s)\,\gamma_n(z_r) K_n\, r} \times \sum_4 \left\{ \cos\left[\frac{2\pi\,(r \pm r_s \pm r_r)}{r_c} j \right] \right\}. \tag{12}$$

Finally combining Eqs. (5) and (12) for P_1 and P_2, P becomes

$$\begin{aligned} P &= \frac{2\pi}{4} \sum_n \frac{{A_n}^4}{\gamma_n(z_s)\,\gamma_n(z_r) K_n r} \times \left(1 + 2 \sum_j \sum_4 \frac{1}{4} \left\{ \cos\left[\frac{2\pi\,(r \pm r_s \pm r_r)}{r_c} j \right] \right\} \right) \\ &= \frac{2\pi}{16} \sum_n \frac{{A_n}^4}{\gamma_n(z_s)\,\gamma_n(z_r) K_n r} \times \left(\sum_4 \left\{ 1 + 2 \sum_j \cos\left[\frac{2\pi\,(r \pm r_s \pm r_r)}{r_c} j \right] \right\} \right). \end{aligned} \tag{13}$$

Having taken care to retain modal differences already the summation over n can safely be assumed to contain no further significant (large scale) fluctuations. Therefore, following earlier approaches (Harrison, 2003; Harrison and Ainslie, 2010), the sum is treated as a continuum first in n, then K, then ray angle at the source θ_s, using $K = k(z_s)\cos\theta_s$. Thus, substituting for the mode normalization A_n [Eq. (A9)] and using the relation Eq. (A10) for dn/dK, leads to

$$\begin{aligned} P &= \int \frac{K}{\gamma(z_s)\gamma(z_r)\, r_c r} \times \left(\sum_4 \left\{ 1 + 2 \sum_j \cos\left[\frac{2\pi(r \pm r_s \pm r_r)}{r_c} j \right] \right\} \right) dK \\ &= \int \frac{1}{\tan\theta_r\, r_c r} \times \left[\sum_4 \left(1 + 2 \sum_j \cos\left\{ \frac{2\pi[r \pm r_s(\theta_s) \pm r_r(\theta_s)]}{r_c(\theta_s)} j \right\} \right) \right] d\theta_s. \end{aligned} \tag{14}$$

This representation of coarse scale modal interference is the starting point for the three following solution methods: (1) range-averaged eigenrays, (2) depth-averaged eigenrays, and (3) a more efficient pre-summed cosine formula.

B. Representation as a sum of eigenrays

Regardless of the angle dependence of the cosine argument in Eq. (14) this first order formula is linear in j and so it can be summed analytically for a given finite upper limit N, and it can also be solved for an infinite upper limit by using the Poisson sum formula (Morse and Feshbach, 1953, pp. 1092–1100). In fact the summation over j is a summation over mode number *differences* [see Eq. (12) cf. Eq. (11)] and, thinking of the cross terms as a $M \times M$ matrix, where M is the number of modes permitted by the water column, clearly the upper limit of j ($=n - m$) is not a fixed constant. Nevertheless, the second order expansion, being proportional to j^2, might be expected to introduce an effectively constant limit on j (i.e., a fixed distance from the matrix's diagonal) that is often much smaller than the true number of modes M.

The analytical sum is shown in Appendix C to be

$$\sum_{j=1}^{N} \cos(Xj) = \frac{\sin[(N+1)X/2]}{\sin(X/2)} \cos(NX/2) - 1 \tag{15}$$

and by allowing N to tend to infinity or by using the Poisson sum formula (Appendix B), it can be shown that the right hand side becomes a row of delta functions in X with separation $2\pi m$,

$$\begin{aligned} 1 + \sum_{j=1}^{\infty} 2\cos(Xj) &= \sum_{j=-\infty}^{\infty} \exp(iXj) \\ &= \sum_{m=-\infty}^{\infty} 2\pi\,\delta(X + 2\pi m). \end{aligned} \tag{16}$$

By comparing this with Eq. (14) where

$$X = \frac{2\pi[r \pm r_s(\theta_s) \pm r_r(\theta_s)]}{r_c(\theta_s)}, \tag{17}$$

it can be seen that the delta function locations are given by

$$r = m\, r_c(\theta_s) \mp r_s(\theta_s) \mp r_r(\theta_s) \tag{18}$$

and correspond exactly to eigenrays with the integer m representing the number of full ray cycles. A similar link from modes to ray theory is shown in Brekhovskikh and Lysanov (2003, p. 140–143) and Haskell (1951). Substituting the delta functions in Eq. (14) leads to

$$P = \int \frac{1}{\tan\theta_r\, r_c r} \left[\sum_4 \sum_{m=-\infty}^{\infty} 2\pi\,\delta(X + 2\pi m) \right] d\theta_s, \tag{19}$$

which by using the definition of X and the delta function can be written as

$$P = \int \frac{1}{\tan\theta_r r_c r}\left\{\sum_4\left[\sum_{m=-\infty}^{\infty} 2\pi\delta(X+2\pi m)\right]\right\} \times \frac{d\theta_s}{d(2\pi r/r_c)}\, d(2\pi r/r_c) = \int \frac{1}{\tan\theta_r r}\left[\sum_4\left(\sum_{m=-\infty}^{\infty}\frac{d\theta_s}{dr}\right)\right]. \quad (20)$$

It is interesting to compare this with the standard power-down-a-ray-tube formula (see Brekhovskikh and Lysanov, 2003, p. 45).

$$E = \frac{\cos\theta_s}{r\sin\theta_r\,|\frac{dr}{d\theta_s}|}. \quad (21)$$

When converted to ratio-of-pressure-squared by allowing for the impedance difference at source and receiver (assuming uniform density and sound speeds c_s and c_r), this becomes

$$P = \frac{c_r}{c_s}\frac{\cos\theta_s}{r\sin\theta_r\,|\frac{dr}{d\theta_s}|} = \frac{1}{r\tan\theta_r\,|\frac{dr}{d\theta_s}|}.$$

On summing over all eigenrays, this is identical to Eq. (21).

III. USABLE FORMULAS

A. Gaussian running range average

Although it is gratifying to see the agreement in Eq. (21) between simple ray flux and the original mode formulation, the derivation is not new, and also the formulation leads to all the well known housekeeping problems of ray tracing (Jensen *et al.*, 1994, pp. 155–185). As an alternative a local range average [of Eq. (19)] can be set up to integrate in r over nearby delta functions but retain the angle integral and the quantities r_c, r_s, r_r which are all functions of angle. The normalized range average is assumed to be Gaussian weighted, of width p and centered on range r_o, (explicitly excluding the cylindrical spreading in the averaging)

$$P(r_o) = \int \frac{1}{\tan\theta_r r_c r_o}\frac{1}{p\sqrt{\pi}}\int \exp[-(r-r_o)^2/p^2] \times\left\{\sum_4\left[\sum_{m=-\infty}^{\infty} 2\pi\delta(X+2\pi m)\right]\right\} dr\, d\theta_s = \frac{1}{r_o}\frac{1}{p\sqrt{\pi}}\int\frac{1}{\tan\theta_r}\sum_4\left[\sum_{m=-\infty}^{\infty}\exp\left(-\{[mr_c(\theta_s) \pm r_s(\theta_s)\pm r_r(\theta_s)]-r_o\}^2/p^2\right)\right] d\theta_s. \quad (22)$$

This equation appears to suffer from the raytracing problem that there is a singularity at ray turning points when $\theta_r = 0$. However, the denominator can be traced back to Eq. (14) where the denominator of the WKB mode [Eq. (A2)] appears as $\gamma(z_s)$ and $\gamma(z_r)$. This can be rectified by substituting an Airy function in this region for the WKB solution (see Morse and Feshbach, 1953, p. 1098), and in the interests of fast computer code one can use the crude but simple trick of truncating the WKB amplitude with a frequency-dependent ceiling value (Harrison, 2011a, p. 6). Thus $(1/\tan\theta_r)$ $[= (c_r/c_s)(\cos\theta_s/\sin\theta_r)]$ reverts to $(\cos\theta_r \sin\theta_s k_s k_r)/(\gamma_s\gamma_r)$ [see Eq. (14)], where subscripts s,r denote the quantities at source and receiver depths, respectively, and the WKB denominators (i.e., $1/\tan\theta_r$) are replaced as follows:

$$\cos\theta_r\sin\theta_s\left\{MIN\left(\frac{1}{\sin\theta_s}, k_s B_s\right)\right\}\left\{MIN\left(\frac{1}{\sin\theta_r}, k_r B_r\right)\right\},$$

where

$$B_{s,r} = \left[\frac{2}{3\pi|d(k^2)/dz|_{s,r}|}\right]^{1/3}.$$

B. Range-varying depth average

Although rays may converge and diverge the intensity averaged across the entire depth can only decay monotonically as cylindrical spreading (ignoring losses) as is shown in Appendix D. Here the normalized Gaussian weighted average is adapted to be a vertical depth average of width q centered on depth z_o. Thus the depth average of Eq. (19) becomes

$$P = \int \frac{1}{\tan\theta_r r_c r}\frac{1}{q\sqrt{\pi}}\int \exp\{-(z-z_o)^2/q^2\} \times\left\{\sum_4\left\{\sum_{m=-\infty}^{\infty} 2\pi\delta(X+2\pi m)\right\}\right\} dz\, d\theta_s. \quad (23)$$

But according to Eq. (17) $X = \{2\pi[r \pm r_s(\theta_s) \pm r_r(\theta_s)]\}/r_c(\theta_s)$ so

$$\int \delta(X+2\pi m)\, dr_r\, 2\pi/r_c = 1. \quad (24)$$

Therefore, the integral in z becomes

$$\int \delta(X+2\pi m)F(z)dz = \int \delta(X+2\pi m)F(z)\frac{dz}{dr_r}dr_r = F(z_r)\frac{r_c}{2\pi}\frac{dz}{dr_r} = F(z_r)\frac{r_c}{2\pi}\tan\theta_r, \quad (25)$$

where F is an arbitrary function of z, and z_r means the depth at which the ray arrives given the current launch angle θ_s and the range r. So Eq. (23) becomes

$$P = \frac{1}{r}\frac{1}{q\sqrt{\pi}}\int\left(\sum_4\left\{\sum_{m=-\infty}^{\infty}\exp[-(z_r-z_o)^2/q^2]\right\}\right)d\theta_s. \quad (26)$$

Although this looks simple, z_r has to be determined from r_c and r_s given the current range which is the inverse of the

usual procedure of finding the range given the receiver depth.

C. Analytically summed version of the cosine sum

It is shown in Appendix C that a good approximation to the cosine sum in the inner curly brackets of Eq. (14) is

$$1+2\sum_{j=1}^{N}\cos(Xj)\approx(1+2N)\times\exp\left[-\frac{(1+2N)^2}{\pi}\sin(X/2)^2\right], \tag{27}$$

where N is an effective number of modes (to be discussed in Sec. III D). So the coherent pressure-squared becomes

$$P(r)=\int\frac{1}{\tan\theta_r r_c r}\left\{\sum_4\left[(1+2N)\exp\left(-\frac{(1+2N)^2}{\pi}\times\sin^2\left\{\frac{2\pi\left[r\pm r_s(\theta_s)\pm r_r(\theta_s)\right]}{2\times r_c(\theta_s)}\right\}\right)\right]\right\}d\theta_s. \tag{28}$$

With the exception of the summation over four terms, this has reduced to just the angle integral which implies the same order of computation time as the incoherent sum [see Eq. (1) when converted to an angle integral or Harrison and Ainslie, 2010, Eqs. (B3) and (B8)].

D. The relation between the effective number of modes *N* and the waveguide invariant *β*

It is clear in all the formulas [Eqs. (22), (26), and (28)] that variation of r_c, r_s, r_r with angle in the integral will smudge the peaks or convergences. Furthermore, reducing N in Eq. (28) will also broaden the peaks.

A second order Taylor expansion of each cosine in the sum can be written as

$$\sum_{j=-\infty}^{\infty}\exp(iAj)\exp(iBj^2) \tag{29}$$

with

$$A\equiv-2\pi(r\pm r_s\pm r_r)/r_c, \tag{30}$$

$$B\equiv\frac{\pi}{r_c}\times\frac{d}{dK}\left[\frac{2\pi(r\pm r_s\pm r_r)}{r_c}\right]. \tag{31}$$

Appendix B shows that there is a width $(r_c/\pi)\sqrt{|B|}$ associated with the second order Taylor expansion. Comparing it with the width $r_c/(\pi N)$ caused by the finite number of terms N in Eq. (C5), the effective number of modes can be seen to be $N\sim|B|^{-1/2}$. In the first order Taylor expansion B is 0, and [before angle integration, Eq. (14)] there is perfect focusing with constant cycle distance. The second order term allows for cycle distance to increase or decrease with angle. This is reminiscent of the behavior of the waveguide invariant β (Chuprov, 1982) as seen from the point of view of a multipath impulse response (Harrison, 2011b): for a perfectly focusing duct (cosh profile) β tends to infinity; for cycle distance decreasing with angle β is positive, and for cycle distance increasing with angle β is negative. In particular, β is $+1$ for isovelocity and -3 for the upward refracting duct considered later in this paper. It is shown in Appendix B that, in fact, B is directly related to the waveguide invariant β by

$$B=-\frac{\pi r}{r_c\beta M}. \tag{32}$$

Therefore, the number of terms in the sum, or the effective number of modes, is

$$N=\frac{1}{\sqrt{|B|}}=\sqrt{\frac{r_c|\beta|M}{\pi r}}=\sqrt{\frac{|\beta|M}{\pi m}}, \tag{33}$$

where M is the actual number of modes and m is the number of ray cycles. Similarly, the ratio ν of number of effective to actual modes is

$$\nu=\sqrt{\frac{|\beta|}{\pi mM}}. \tag{34}$$

E. The relation between the effective number of modes *N* and the horizontal smoothing width *p*

Comparing the range average, Eq. (22) with Eq. (28) [which is an approximation to the cosine sum, Eq. (14)] it can be seen that they are very similar in form near the peaks. In fact, the numerators and exponents can be made identical near the peaks by putting

$$1+2N=r_c/(p\sqrt{\pi}). \tag{35}$$

So for large N there is a rough equivalence between the number of terms N (i.e., effective number of modes) and the reciprocal of range averaging window size p.

The equivalence when p is small compared with r_c implies that the range average [Eq. (22)] can also be written as the more efficient computation

$$P(r)=\int\frac{1}{\tan\theta_r r}\frac{1}{p\sqrt{\pi}}\left\{\sum_4\left[(1+2N)\exp\left(-\frac{{r_c}^2}{\pi^2p^2}\times\sin^2\left\{\frac{2\pi\left[r\pm r_s(\theta_s)\pm r_r(\theta_s)\right]}{2\times r_c(\theta_s)}\right\}\right)\right]\right\}d\theta_s. \tag{36}$$

For p approaching, or larger than, r_c one needs to revert to Eq. (22), or alternatively to regard Eq. (36) still as a range average with a "characteristic width" p but with a modified weighting function.

F. The relation between the actual mode number *M* and the vertical smoothing width *q*

One might expect the vertical and horizontal averaging to be similarly blurred if one sets $q/p\sim\tan\theta$ which, on substituting for p leads to $q\sim\tan\theta\, r_c/(N\pi)\sim(2H)/(N\pi)$. On

the other hand, the vertical resolution of a mode sum is set by the vertical correlation length (a fraction of the vertical wavelength) of the highest mode which is roughly related to water depth H by $H/(M\pi)$.

G. Extension to range-dependent environments

Though not tackled in this paper, it is interesting to note that handling range-dependent environments using this approach is quite straightforward. If Eq. (1) were based on the adiabatic mode sum the cross terms would have contained integrals of wave number over range whose differences would have appeared as

$$\exp\left[i\left(\int K_n dr - \int K_m dr\right)\right] = \exp\left(i\int \frac{2\pi}{r_c} dr\, j\right). \quad (37)$$

So Taylor expansions are still possible but the argument of the sine term in Eq. (28) becomes range-dependent when r_c is range-dependent. In fact the ray cycle distance can be seen to function as a "period" in the sine term when the two partial cycle distances (r_s and r_r), evaluated, respectively, at source and receiver ranges, act as "phases."

IV. SUMMARY OF SOLUTIONS

Three potentially useful solutions have been derived, each showing slightly different but very similar ray convergence behavior.

(1) Running range average (smoothing length p)

$$P(r) = \frac{1}{rp\sqrt{\pi}} \times \int \frac{1}{\tan\theta_r} \sum_4 \left[\sum_{m=-\infty}^{\infty} \exp(-\{[mr_c(\theta_s) \pm r_s(\theta_s) \pm r_r(\theta_s)] - r\}^2/p^2) \right] d\theta_s. \quad (22)$$

(2) Running range average hybrid for $p \lesssim r_c$

$$P(r) = \int \frac{1}{\tan\theta_r r} \frac{1}{p\sqrt{\pi}} \left\{ \sum_4 \left[(1+2N)\exp\left(-\frac{{r_c}^2}{\pi^2 p^2} \times \sin^2\left\{ \frac{2\pi\,[r \pm r_s(\theta_s) \pm r_r(\theta_s)]}{2 \times r_c(\theta_s)} \right\} \right) \right] \right\} d\theta_s. \quad (36)$$

Although this formula is shown explicitly here for completeness, it does not constitute a separate solution since it is merely Eq. (28) with the substitution Eq. (35).

(3) Range-varying depth average (smoothing depth q)

$$P(r,z_o) = \frac{1}{r} \frac{1}{q\sqrt{\pi}} \int \left(\sum_4 \left\{ \sum_{m=-\infty}^{\infty} \exp[-(z_r - z_o)^2/q^2] \right\} \right) d\theta_s. \quad (26)$$

(4) Analytical cosine sum (effective number of modes N)

$$P(r) = \int \frac{1}{\tan\theta_r r_c r} \left\{ \sum_4 \left[(1+2N)\exp\left(-\frac{(1+2N)^2}{\pi} \times \sin^2\left\{ \frac{2\pi\,[r \pm r_s(\theta_s) \pm r_r(\theta_s)]}{2 \times r_c(\theta_s)} \right\} \right) \right] \right\} d\theta_s. \quad (28)$$

All formulas need to be integrated over angle, as shown. Both the range average and the depth average contain an extra summation compared with the analytical cosine sum (and the range average hybrid). When compared with propagation calculations based on the incoherent sum (see e.g., Harrison, 2003; Harrison and Ainslie, 2010; Harrison, 2011a) the angle integral in Eq. (28) has simply substituted the term in the outer curly brackets with no change to the angle integration scheme or to the term $1/(rr_c\tan\theta_r)$. It is true that this new formula requires complete and partial cycle distances as a function of angle, but these can be tabulated beforehand. In a practical implementation such as Artemis (Harrison, 2011a) much of the computational effort goes into calculating the boundary losses. Although ignored in this paper, this inevitable computational overhead makes the additional computation time due to convergence effects even less significant.

The range average is straightforward to implement given complete and partial cycle distances as a function of angle, but the depth average is slightly more difficult. This is because, given a source depth, a receiver depth, and a sound speed profile (SSP), one can immediately calculate r_s and r_r, but given a receiver range r, it is possible, but more complicated, to calculate the depth z_r at which the ray arrives. All SSPs considered here are piecewise linear so this "receiver depth inversion" can be done without requiring interpolation.

As discussed in Sec. III A a standard problem with WKB modes is that there is a singularity at the depth of the source (and its complementary depth) (Weston, 1980c). This is tackled here (in the running range average and the analytical cosine sum) in the same way as in the incoherent Artemis—essentially the transition region between the Airy function and WKB is approximated by imposing a frequency-dependent (and SSP-dependent) ceiling value on the WKB function (see Harrison, 2011a, p. 6).

In the running range average if the set of receiver depths and source angles is sparse then there may be a lack of data points (essentially ray arrivals) near ray turning points such that the Gaussian averaging window finds no points. An obvious and fail-safe solution is to increase the averaging window size. An elementary calculation of the worst case data point separation defines the necessary ray density and receiver depth density for the given window size p.

The relation between the three approaches [Eqs. (22), (26), (28)] and the ray intensity shows that, despite the fact that they were all derived from a coherent mode sum, they each bear a strong resemblance to a weighted sum of incoherent rays, which is distinct from an incoherent sum of modes.

V. COMPARISONS BETWEEN THE THREE SOLUTIONS AND THE WAVE MODEL ORCA

Disregarding computation time and computational difficulties, the three formulations of Sec. IV are first evaluated

numerically, and their results compared with each other. Then they are compared with the well established wave model Orca (Westwood *et al.*, 1996). In each case the degree of spatial averaging will also be varied. An upward refracting uniform gradient SSP is taken as the test case. Two other test environments that also exhibit strong convergence were included in Harrison (2012b): a six-point shallow sound channel, and a thousand-point deep Munk profile. The quantity plotted is one-way propagation loss in dB re 1 m.

The upward refracting duct shown in Fig. 1 is chosen because a clear and well known pattern of caustics is expected (see Brekhovskikh and Lysanov, 2003, p. 121). Each caustic line can be thought of as the envelope of the upward curving ray arcs from the source.

A. Three formulations: Fine detail

Each of the three formulations summarized in Sec. IV has a free parameter: for the range average [Eq. (22)], it is the width p; for the depth average [Eq. (26)], it is the width q; for the cosine sum [Eq. (28)], it is N. We expect similar amounts of smoothing if the relations between N, p, and q of Secs. III D to III F are utilized. The number of modes [using, e.g., Eq. (A6)] at frequencies of 100, 1000, 10 000 Hz is 2, 18, 180, so at a high frequency Eq. (33), with $M = 180$, $\beta = -3$, $m = 1$, leads to $N = 13$. To optimize the detail in the illustrations (without introducing spurious pixel sampling issues), N is taken somewhat arbitrarily to be $N = 20$, then this is roughly matched with $p \sim 15$ m according to Eq. (35) and taking r_c to be 1 km, and $q \sim 0.5$ m since there are ~180 modes in 100 m of water. Numerical calculations for the range average, depth average, and cosine sum are shown in Figs. 2(a), 2(b), and 2(c) with, respectively, $p = 15$ m, $q = 0.5$ m, and $N = 20$. The three plots are almost identical, and not surprisingly, there is a strong resemblance to ray

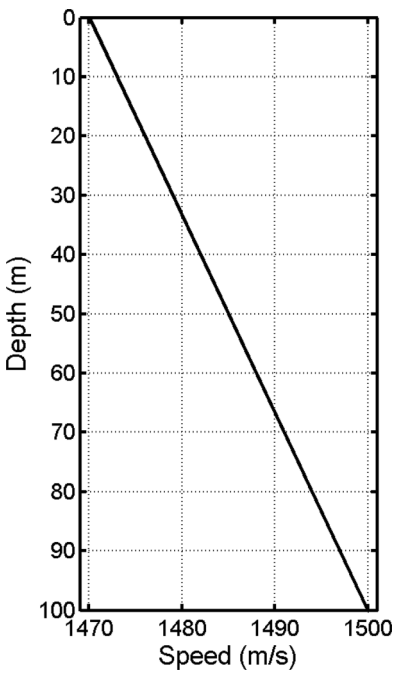

FIG. 1. Sound speed profile (SSP) for the Upward Refracting Linear Duct.

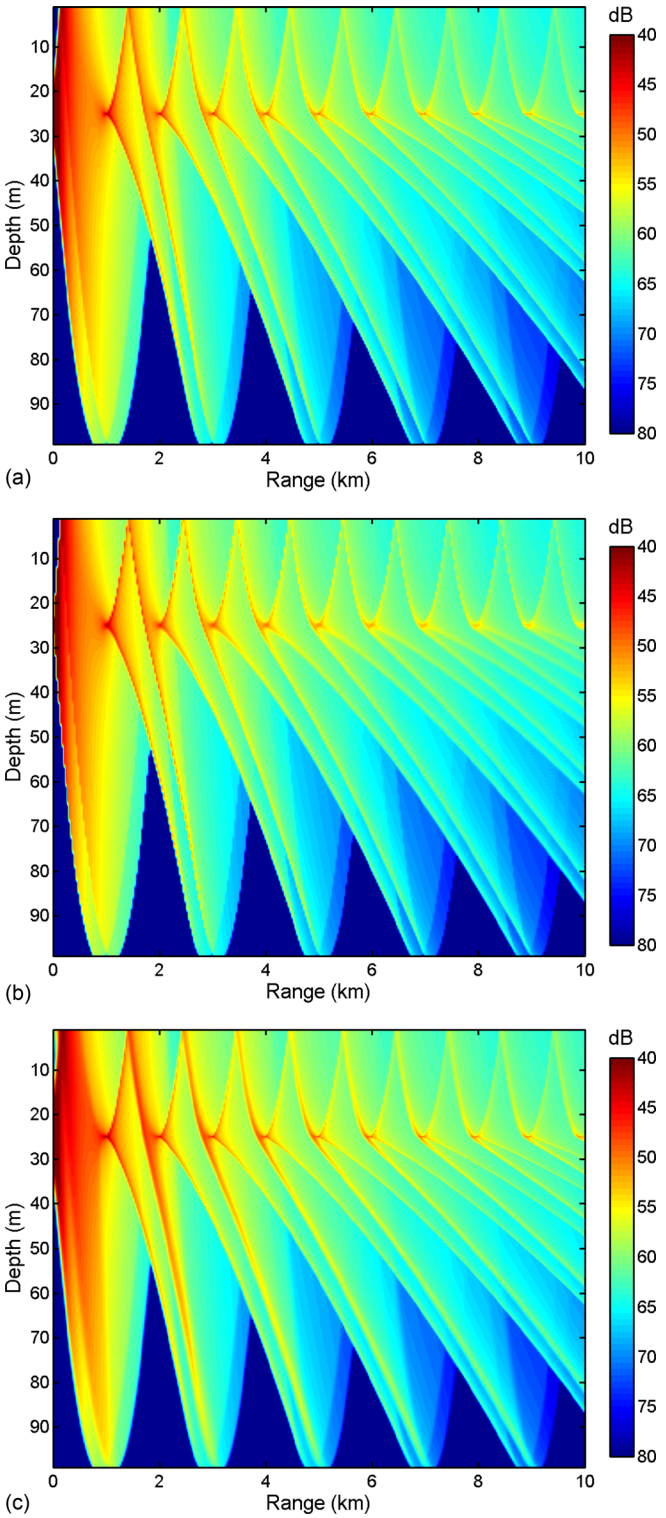

FIG. 2. (Color online) Propagation loss (dB re 1 m) for upward refracting linear SSP with source at depth 25 m, (a) "Running range average," Eq. (22) with $p = 15$ m, (b) "Range-varying depth Average," Eq. (26) with $q = 0.5$ m, and (c) "Analytical cosine sum," Eq. (28) with $N = 20$.

tracing images with clear ray cycling, refraction ducting, bottom reflection, and caustic features. From the first ray cycle on, there is a focus when the receiver is at the source depth, and this is followed by a pair of caustic lines going towards and away from the sea surface. The surface-bound caustic line is then reflected in the surface adding a

descending caustic. This behavior is identical to that shown on p. 121 of Brekhovskikh and Lysanov (2003).

A glance at Eqs. (22), (26), (28), and (36) shows that they are not directly sensitive to frequency, and the effective number of modes N behaves like an independent parameter. Nevertheless with the exception of Eq. (26), the formulas are sensitive to small angles when either the source or the receiver happens to be close to a ray turning point. One solution would be to introduce the frequency-dependent Airy correction to the WKB function as in Sec. III A. Instead, to retain the frequency independence a simple angle limit of 0.01 rad was used throughout.

B. Comparison with Orca

The Orca results for the upward refraction case at 10 kHz and 1 kHz are shown in Figs. 3(a) and 3(b). The most noticeable difference between these plots and the three solutions in Figs. 2(a), 2(b), and 2(c) is the fine fringes of the interference patterns. This interference is exactly what has been deliberately left out in the solutions derived here—to be precise, it is the step between Eqs. (7) and (8) where the $\cos[w_n(z_{s,r}) + w_m(z_{s,r})]$ terms were rejected. Otherwise the general picture of shadow zones, convergences, caustics, and refraction is identical.

C. Three formulations: Medium detail

To make a fairer comparison, one can apply wider averaging windows to the three formulas and to Orca: a range average, Eq. (22) with $p = 300$ m, is shown in Fig. 4(a), and a depth average, Eq. (26) with $q = 10$ m, is shown in Fig. 4(b). The ray cycling behavior is still visible in each although the details are different.

D. Numerical range and depth averages of Orca

A numerical range and depth average of the 10 kHz Orca result of Fig. 3(a) is shown in Fig. 5(a) and 5(b). There is a strong resemblance between the two range averages [Figs. 4(a) and 5(a)] and the two depth averages [Figs. 4(b) and 5(b)] but not so much between all four, which is not surprising—they are different quantities.

E. Comparison of range-varying depth average

Although the plots of propagation loss against range and depth show that the main features of all three proposed

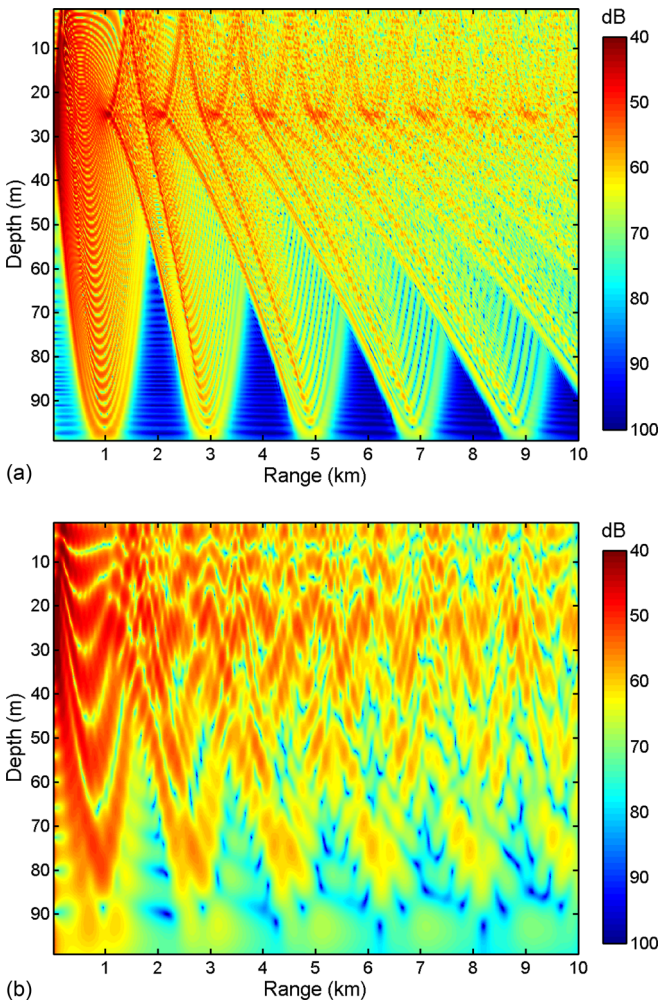

FIG. 3. (Color online) Propagation loss (dB re 1 m) for the upward refracting linear SSP with source at depth 25 m using the wave model Orca at (a) 10 kHz, (b) 1 kHz.

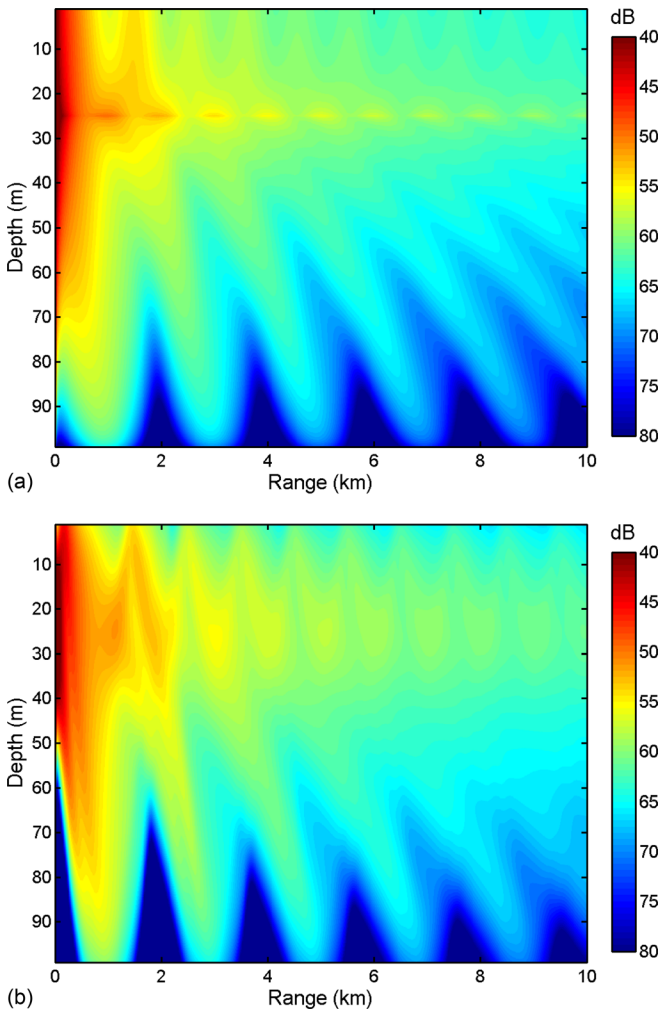

FIG. 4. (Color online) Analytically smoothed propagation loss for (a) "Running range average," Eq. (22) with $p = 300$ m, (b) "Range-varying depth Average," Eq. (26) with $q = 10$ m.

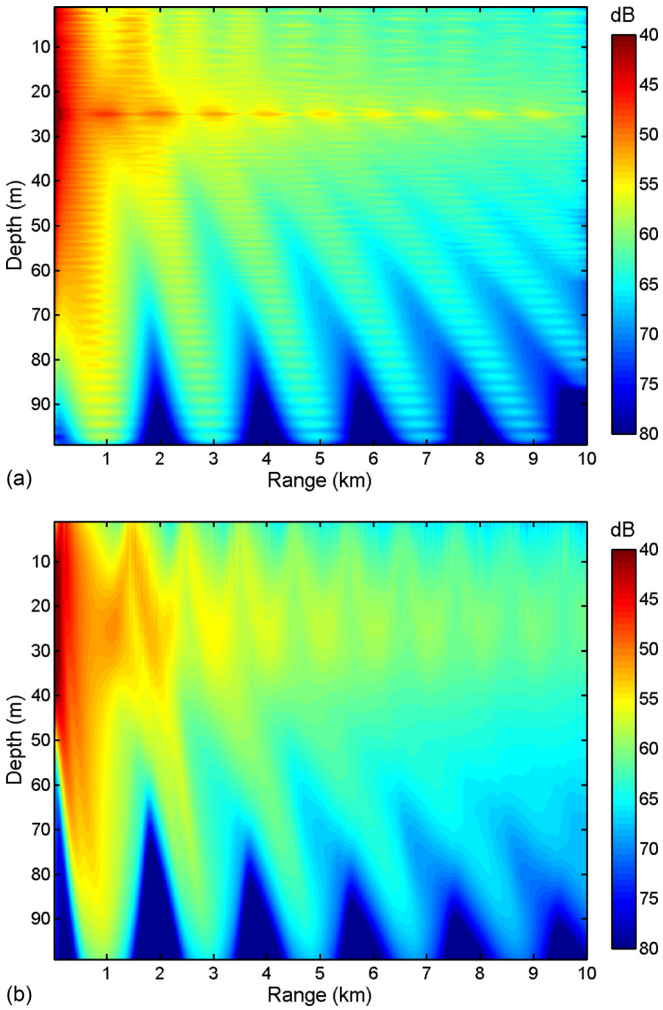

FIG. 5. (Color online) Numerical average of Orca wave solution at 10 kHz: (a) on a range scale of 300 m, and (b) on a depth scale of 10 m.

methods agree well with Orca, a more quantitative comparison is obtained by taking slices at fixed ranges and plotting these against depth. For this purpose the slices are taken

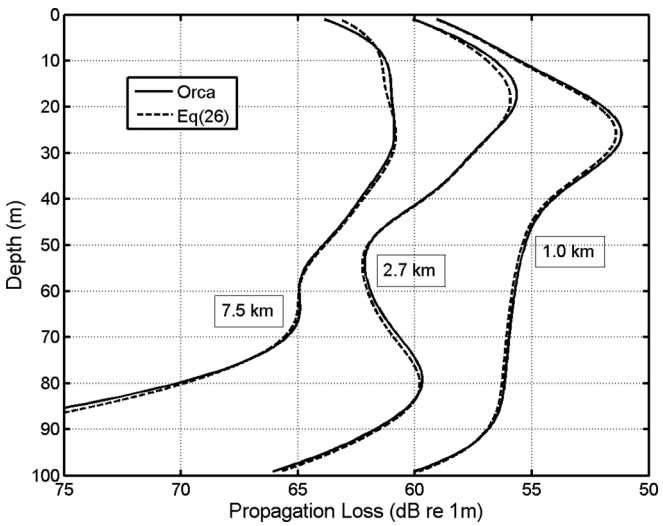

FIG. 6. Comparison between range-varying depth average of Orca (solid) and Eq. (26) (dashed). Slices are taken at fixed ranges of 1.0, 2.7, and 7.5 km through the depth-range surfaces shown in Figs. 5(b) and 4(b), respectively.

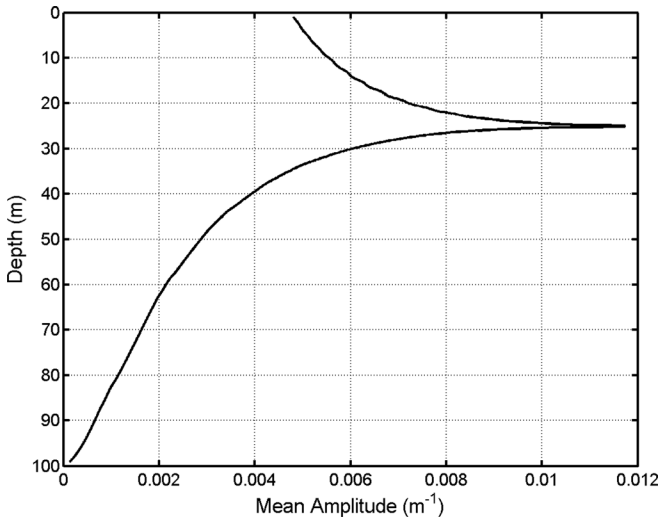

FIG. 7. Range-averaged pressure-squared vs depth [$\langle r\,P(r)\rangle$ from Eq. (28)] with source at 25 m.

from Figs. 4(b) and 5(b) which are equivalently depth averaged. In Fig. 6, three ranges are chosen (1.0, 2.7, 7.5 km) to show examples of peaks and troughs without crowding the graph. The solid lines are Orca and the dashed lines are Eq. (26) all with $q = 10$ m. The fit is extremely good—well within 0.5 dB and centered on the Orca line.

F. Depth plot of range average

In passing, it is interesting to plot the average over all ranges against depth. Figure 7 shows the numerical average over range of $rP(r)$ from Eq. (28) for $N = 20$. Notice the strong peak at the source depth as pointed out by Weston (1980a) and the strong similarity in shape to his "depth factor."

VI. CONCLUSIONS

The ultimate aim of this work is to be able to calculate reverberation and target echoes very rapidly in an operational research context where many military scenarios with many possible sonar parameters in many environments need to be evaluated. Consequently there is a need to minimize the number of computer operations in calculating sound propagation. An energy flux or incoherent mode sum approach has been very successful in this respect except that, to date, it is restricted to mode stripping superimposed on cylindrical spreading. This leads to a monotonic decay in range with the possible exception of minor deviations from monotonic in a range-dependent environment.

This paper has derived three formulations from the coherent mode sum: a running range average with variable window width p; a range-varying depth average with variable width q; and an analytical cosine sum with parameter N equal to the number of terms in the sum. This number is related to, but a lot less than, the number of water-borne modes. An upward refracting linear SSP environment was chosen to demonstrate performance of these formulations. Very similar plots are produced for large N and relatively small p and q. As p and q are increased and N decreased,

they all start to deviate from each other, as one might expect. Comparisons with the wave model Orca run at various frequencies with, and without, averaging show very good agreement allowing for the obvious presence of its interference fringes.

From the point of view of number of computation operations, it is clear from Eq. (28) that the analytical cosine sum consists of the same integral over angle as in the Artemis implementation of the incoherent mode sum. The only difference is that the integrand is more complicated and that it includes the partial ray cycle distances from the source and receiver depths as well as the complete cycle distance. In this respect the computation time of Artemis will not be compromised by substituting this formulation for convergence.

As a by-product the derivation has shown that a running range average [Eq. (22)] is always extremely close to the analytical cosine sum [Eq. (28)] given the relation (Sec. III E) between averaging window size and number of terms in the sum, which, in turn, is the effective number of modes. This effective number is usually much smaller than the actual number and depends on the variation of ray cycle distance (or mode separation in wave number) with angle. The effective number was shown to be closely related to the waveguide invariant. Both solutions are close to the mode solution at any reasonably high frequency with the interference fringes taken out.

An interesting observation is that the three solutions-with-convergence bear strong resemblance to an incoherent ray sum—Eq. (21) explicitly represents power-down-a-ray-tube, and the other formulas are just the power sum of terms like this. Although this was derived from the modulus square of the coherent mode sum, it is distinctly different from the incoherent mode sum that does include mode stripping but does not include convergence.

ACKNOWLEDGMENT

This work was funded by ONRG under grant number N62909-12-1-7029. The author is indebted to Dr. Peter Nielsen for running the propagation model Orca on the test cases.

APPENDIX A: DEFINITIONS

1. WKB modes

The acoustic intensity at depth z_r and range r with a source at depth z_s in a range-independent medium can be written in terms of its normal modes $\phi_n(z)$ with eigenvalues K_n as

$$\begin{aligned} P &= 2\pi\left|\sum_n \frac{\phi_n(z_s)\,\phi_n(z_r)\exp(iK_n r)}{\sqrt{K_n r}}\right|^2 \\ &= 2\pi\sum_n \frac{{\phi_n}^2(z_s)\,{\phi_n}^2(z_r)}{K_n r} \\ &\quad + 2\pi\sum_m\sum_n \frac{\phi_n(z_s)\,\phi_n(z_r)\,\phi_m(z_s)\,\phi_m(z_r)}{\sqrt{K_n K_m}\,r} \\ &\quad \times \cos[(K_n - K_m)r]. \end{aligned} \tag{A1}$$

The relations below follow from the Appendix in Harrison and Ainslie [2010, Eqs. (B3) and (B8)]. Wenzel-Kramers-Brillouin (WKB) modes are assumed

$$\phi_n = A_n \frac{\sin\left[\int_{z_B}^{z_s}\sqrt{k^2(z) - {K_n}^2}\,dz - \varepsilon\right]}{[k^2(z) - {K_n}^2]^{1/4}}, \tag{A2}$$

which may be normalized by setting

$$\int {\phi_n}^2(z)\,dz = 1 = \frac{1}{2}\int \frac{{A_n}^2}{[k^2(z) - {K_n}^2]^{1/2}}\,dz = \frac{{A_n}^2}{2}L \tag{A3}$$

introducing the term L,

$$L = \int \frac{1}{[k^2(z) - {K_n}^2]^{1/2}}\,dz \tag{A4}$$

so that ${A_n}^2 = 2/L$,

$${\phi_n}^2(z) = \frac{1}{[k^2(z) - {K_n}^2]^{1/2}} \Big/ \int \frac{1}{[k^2(z) - {K_n}^2]^{1/2}}\,dz. \tag{A5}$$

Differentiating the phase integral (Morse and Feshbach, 1953, pp. 1092–1100)

$$\pi(n - \varepsilon) = \int_0^H \sqrt{k^2(z) - {K_n}^2}\,dz \tag{A6}$$

leads to

$$\frac{dn}{dK} = -\frac{K}{\pi}\int \frac{1}{[k^2(z) - {K_n}^2]^{1/2}}\,dz = -\frac{K}{\pi}L. \tag{A7}$$

Also, by definition, the ray cycle distance is

$$r_c = 2\int \frac{K}{[k^2(z) - K^2]^{1/2}}\,dz = 2KL. \tag{A8}$$

Thus the mode normalization, the inverse of mode separation [i.e., $(dK/dn)^{-1}$], and ray cycle distance are related through the integral L. Particularly useful relations are

$${A_n}^2 = 4K_n/r_c, \tag{A9}$$

$$\frac{dn}{dK} = -\frac{r_c}{2\pi}. \tag{A10}$$

APPENDIX B: TAYLOR EXPANSIONS AND POISSON SUM FORMULA

1. Taylor expansions

Each cosine term in Eqs. (11) and (12), when summed and expanded to second order, is of the form

$$\sum_{j=-\infty}^{\infty} \exp(iAj)\exp(iBj^2). \tag{B1}$$

The three differences constituting the argument of the cosines are Taylor expanded as follows. The first is

$$K_n - K_m = j\frac{dK}{dn} + \frac{j^2}{2}\frac{d^2K}{dn^2} + \cdots \tag{B2}$$

where $j = n - m$ and

$$\frac{dK}{dn} = -\frac{2\pi}{r_c}. \tag{B3}$$

Similarly, the second and third are

$$w_n(z_{s,r}) - w_m(z_{s,r}) = j\frac{dw}{dn} + \frac{j^2}{2}\frac{d^2w}{dn^2} + \cdots \tag{B4}$$

and since

$$w_n(z_o) = \int_{z_B}^{z_o} \sqrt{k^2(z) - K_n{}^2}\, dz - \varepsilon_B, \tag{B5}$$

$$\frac{dw}{dn} = \frac{dw}{dK}\frac{dK}{dn} = \int_{z_B}^{z_{s,r}} \frac{K}{\left[k^2(z) - K^2\right]^{1/2}}\, dz\, \frac{2\pi}{r_c} \tag{B6}$$

and this remaining integral is just the partial cycle distances $r_{s,r}$ from the lower ray turning point to either the source or receiver depth. So

$$\frac{dw(z_{s,r})}{dn} = \frac{2\pi\, r_{s,r}}{r_c}. \tag{B7}$$

Thus, the first order term in the exponent of Eq. (B1) is $A \equiv -2\pi(r \pm r_s \pm r_r)/r_c$, and the sum over the four permutations of $\cos(a \pm b \pm c)$ as in Eq. (11) becomes

$$\sum_4 \cos\left[\frac{2\pi(r \pm r_s \pm r_r)}{r_c}\, j\right].$$

The second order Taylor expansion is just [1/2] d/dn of the first term, i.e.,

$$B \equiv \frac{1}{2}\frac{dA}{dn} = \frac{1}{2}\frac{dA}{dK}\frac{dK}{dn} = -\frac{\pi}{r_c}\frac{dA}{dK}$$
$$= \frac{\pi}{r_c}\frac{d}{dK}\left[\frac{2\pi(r \pm r_s \pm r_r)}{r_c}\right].$$

2. Poisson sum

Having established formulas for A and B in Eq. (B1), if the limits are taken as infinite, the summation can be evaluated using the Poisson sum formula. Felsen (1981) discusses the utility of the Poisson sum in the context of ray-mode equivalence and finding more succinct representations. As stated in Morse and Feshbach (1953) the formula is

$$\sum_{n=-\infty}^{\infty} f(an) = \frac{1}{a}\sum_{m=-\infty}^{\infty} F(2\pi m/a), \tag{B8}$$

where n is an integer and a is an arbitrary constant, while x, K are continuous variables in the Fourier transform pair $f(x)$, $F(K)$ defined as

$$F(K) = \int f(x)\, e^{iKx} dx, \tag{B9}$$

$$f(x) = \frac{1}{2\pi}\int F(K)\, e^{-iKx} dK. \tag{B10}$$

The relevant form of f for first order Taylor expansion is

$$f(x) = \exp(iAx) \Rightarrow \exp(iAn) \tag{B11}$$

so

$$F(K) = \int e^{iAx}\, e^{iKx} dx = 2\pi\, \delta(A + K) \tag{B12}$$

and on setting $a = 1$ in Eq. (B8) and substituting for f and F one finds

$$\sum_{n=-\infty}^{\infty} \exp(iAn) = \sum_{m=-\infty}^{\infty} 2\pi\, \delta(A + 2\pi m). \tag{B13}$$

The relevant form of f for the second order Taylor expansion is

$$f(x) = \exp(iAx)\exp(iB\,x^2) \Rightarrow \exp(iAn)\exp(iB\,n^2) \tag{B14}$$

so

$$F(K) = \int \left(e^{iAx}\, e^{iB\,x^2}\right) e^{iKx} dx = \sqrt{\frac{i\pi}{B}} \exp\left[-i\frac{(A+K)^2}{4B}\right]. \tag{B15}$$

On substituting for f and F in Eq. (B8) again with $a = 1$ one finds

$$\sum_{n=-\infty}^{\infty} \exp(iAn)\exp(iBn^2)$$
$$= \sum_{m=-\infty}^{\infty} \sqrt{\frac{i\pi}{B}} \exp\left[-i\frac{(A + 2\pi m)^2}{4B}\right]. \tag{B16}$$

Comparing Eq. (B16) with (B13), it can be seen that the sequence of delta functions has been replaced with a sequence of Fresnel-type functions, each with width $2\sqrt{B}$ in the quantity A, so if the second order Taylor term is significant then the delta functions are effectively broadened to a certain extent. Because $A \equiv 2\pi(r \pm r_s \pm r_r)/r_c$, this smudging has a width in range r of $(r_c/\pi)\sqrt{B}$.

3. Relation of the second order Taylor term *B* to the waveguide invariant *β*

The waveguide invariant β is a well known parameter that classifies the behavior of the interference fringes with frequency and range (Chuprov, 1982, and many other more recent references). From the point of view of a multipath impulse response Harrison (2011b) derived formulas for β in terms of cycle distance and cycle time, verifying them with a number of special cases. In particular his Eq. (A24) and (A26) can be written as

$$\beta = \frac{r_c{}^2}{2\pi\left(M - \frac{1}{2}\right)} \Big/ \frac{dr_c}{dK}. \tag{B17}$$

Note that for an isovelocity SSP cycle distance decreases with angle, therefore, it increases with K and so, as is well known, β is positive. [The sign is printed ambiguously in Harrison's Eqs. (A24)–(A26).]

Comparing Eq. (B17) with the definition of the second order term B in Eq. (B1) and assuming that r_s, r_r are small compared with r one finds that they are related by

$$B = -\frac{2\pi^2 r}{{r_c}^3}\frac{dr_c}{dK} = -\frac{\pi r}{r_c\,\beta\left(M-\frac{1}{2}\right)}. \tag{B18}$$

So the effective number of modes N (from Sec. III D) for large M is

$$N = \frac{1}{\sqrt{|B|}} = \sqrt{\frac{r_c|\beta|M}{\pi r}} = \sqrt{\frac{|\beta|M}{\pi m}}, \tag{B19}$$

where m is the number of ray cycles, and the ratio ν of effective to actual number of modes is

$$\nu = \sqrt{\frac{|\beta|}{\pi mM}}. \tag{B20}$$

APPENDIX C: FAST, ANALYTICALLY PRE-SUMMED COSINE SERIES

The cosine sum [Eq. (14)] can be expanded as a sum of complex exponentials [as in Eq. (29) with $B=0$] which then form a geometric series with the exact solution

$$\sum_{j=1}^{N}\cos(Xj) = \frac{\sin[(N+1)X/2]}{\sin(X/2)}\cos(NX/2) - 1. \tag{C1}$$

This function repeats when $X/2$ is a multiple of 2π, and its peak value is N. The Taylor expansion in X in the vicinity of a peak is

$$\begin{aligned}
&(N+1)\frac{1-[(N+1)X/2]^2/6}{1-(X/2)^2/6}\,[1-(NX/2)^2/2]-1\\
&\quad=(N+1)\left\{1-(X/2)^2\left[\frac{(N+1)^2-1}{6}+\frac{N^2}{2}\right]\right\}-1\\
&\quad=(N+1)\left\{1-(X/2)^2\left[\frac{(2N^2+N)}{3}\right]\right\}-1\\
&\quad=N\left\{1-(X/2)^2\left[\frac{(2N+1)(N+1)}{3}\right]\right\}.
\end{aligned} \tag{C2}$$

For reasonably large N this can be fitted with the slightly smoother function $N\times\exp[-A\sin^2(X/2)]$ which retains the multiple peak, peak height, and peak width behavior. Equating Taylor expansions results in

$$A = \frac{(2N+1)(N+1)}{3}, \tag{C3}$$

and so

$$\begin{aligned}
\sum_{j=1}^{N}\cos(Xj) &= \frac{\sin[(N+1)X/2]}{\sin(X/2)}\cos(NX/2)-1\\
&\approx N\exp\left[-\frac{(2N+1)(N+1)}{3}\sin^2(X/2)\right].
\end{aligned} \tag{C4}$$

Retaining the correct peak value of $2N+1$ and the mean of zero in between peaks in Eq. (14) requires

$$\begin{aligned}
&1+2\sum_{j=1}^{N}\cos(Xj)\\
&\quad\approx(1+2N)\exp\left[-\frac{(2N+1)(N+1)}{3}\sin^2(X/2)\right].
\end{aligned} \tag{C5}$$

Notice that the 1 on the left hand side represents the incoherent sum; the true solution in Eq. (C1) oscillates in between peaks and may take values above or below the incoherent sum. On the right of Eq. (C5) the 1 no longer represents the incoherent sum, it is merely ensuring a correct peak value.

Other peak width compromises are possible, for instance one can put $A=N^2$ which leads to

$$1+2\sum_{j=1}^{N}\cos(Xj)\;\approx(1+2N)\exp[-N^2\sin^2(X/2)]. \tag{C6}$$

In the current context, the peaks in the exponential function behave like broadened delta functions, so it is their integral that should be equated to the integral of the exact form in Eq. (C1). Since $\int_0^{2\pi}\{\sin[(N+1)X/2]/\sin(X/2)\}\cos(NX/2)dX=2\pi$ [as may be shown by integrating both sides of Eq. (C1)], one finds

$$\begin{aligned}
1+2\sum_{j=1}^{N}\cos(Xj)\;&\approx(1+2N)\\
&\times\exp\left[-\frac{(2N+1)^2}{\pi}\sin^2(X/2)\right].
\end{aligned} \tag{C7}$$

The four expressions: Eqs. (C1), (C5), (C6), and (C7) are shown in Fig. 8.

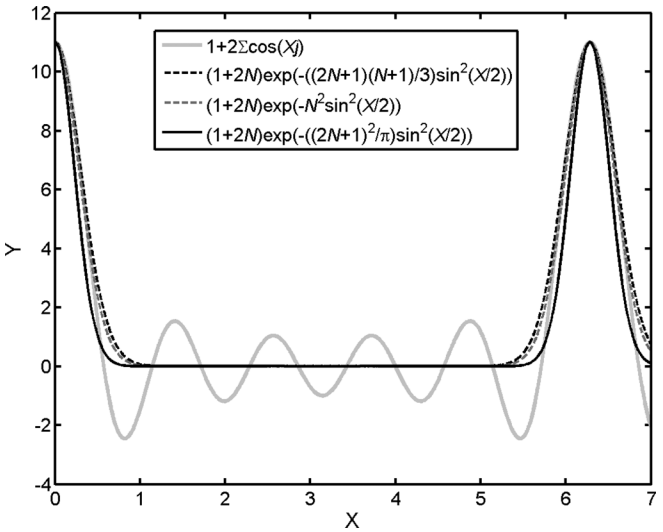

FIG. 8. Comparisons between the cosine sum of Eq.((C1)) (thick gray), the Taylor expansion formula of Eq. (C5) (black dashed), the simpler compromise peak width formula of Eq. (C6) (gray dashed), and the integral-of-peaks formula of Eq. (C7) (black solid), all for $N=5$. The peak value for all formulas is $2N+1=11$ in this case. The second peak occurs at $X=2\pi$.

APPENDIX D: AVERAGE OVER ENTIRE DEPTH

In this appendix three quantities are evaluated and shown to have the same (cylindrical spreading) range dependence. Strictly these are ratios of mean-square-pressure at the source and receiver and differ from true intensity by a factor of the ratio of impedances which is very close to unity for angles of sonar interest.

1. The incoherent mode sum

$$P = 2\pi \sum_n \frac{\phi_n{}^2(z_s)\,\phi_n{}^2(z_r)}{K_n r}. \tag{D1}$$

2. Depth average of the incoherent mode sum

$$\langle P \rangle = \int_0^H P(z_r)\,dz_r = 2\pi \sum_n \frac{\phi_n{}^2(z_s) \int_0^H \phi_n{}^2(z_r)\,dz_r}{K_n r}$$
$$= 2\pi \sum_n \frac{\phi_n{}^2(z_s)}{K_n r}. \tag{D2}$$

3. Depth average of the coherent mode sum

The coherent mode sum is

$$P = 2\pi \sum_n \frac{\phi_n{}^2(z_s)\,\phi_n{}^2(z_r)}{K_n r} + 2\pi \sum_m \sum_n \frac{\phi_n(z_s)\,\phi_n(z_r)\,\phi_m(z_s)\,\phi_m(z_r)}{\sqrt{K_n K_m}\, r} \times \cos[(K_n - K_m) r]. \tag{D3}$$

The depth integral of the first term is exactly the same as Eq. (D2), but the depth integral of the second term

$$P_2 = 2\pi \sum_m \sum_n \frac{\phi_n(z_s)\,\phi_m(z_s) \int_0^H \phi_n(z_r)\;\phi_m(z_r) dz_r}{\sqrt{K_n K_m}\, r} \times \cos[(K_n - K_m) r] \tag{D4}$$

is exactly 0, by the orthogonality condition. So the depth average of the coherent intensity is the same as the depth average of the incoherent intensity.

As a consequence, regardless of any real focusing and convergence, the depth average (when multiplied up by $2\pi r$) is range-invariant—in a loss-free environment all the sound goes somewhere—at each range, convergence at one depth is balanced by divergence at another.

Baggeroer, A. B., Scheer, E. K., Heaney, K., D'Spain, G., Worcester, P., and Dzieciuch, M. (**2010**). "Reliable acoustic path and convergence zone bottom interaction in the Philippine Sea 09 Experiment (A)," J. Acoust. Soc. Am. **128**, 2385.

Beilis, A. (**1983**). "Convergence zone positions via ray-mode theory," J. Acoust. Soc. Am. **74**, 171–180.

Brekhovskikh, L., and Lysanov, Yu. (**2003**). *Fundamentals of Ocean Acoustics*, 3rd ed. (Springer, New York), p. 129.

Chuprov, S. D. (**1982**). "Interference structure of a sound field in a layered ocean," in *Ocean Acoustics, Current Status*, edited by L. M. Brekhovskikh and I. B. Andreyeva (Nauka, Moscow), pp. 71–91, and (Joint Publications Research Service, Washington, DC, 1985), pp. 88–111.

Collins, M. D. (**1993**). "A split-step Padé solution for the parabolic equation method," J. Acoust. Soc. Am. **93**, 1736–1742.

DiNapoli, F. R., and Deavenport, R. L. (**1979**). "Numerical models of underwater acoustic propagation," in *Ocean Acoustics*, edited by J. A. deSanto (Springer-Verlag, Berlin), pp. 79–157.

Felsen, L. B. (**1981**). "Hybrid ray-mode fields in inhomogeneous waveguide ducts," J. Acoust. Soc. Am. **69**, 352–361.

Ferla, C. M., Porter, M. B., and Jensen, F. B. (**1993**). "C-SNAP: Coupled SACLANTCEN normal mode propagation loss model," Memo. Rep. No. SM-274, SACLANT Undersea Research Center, La Spezia, Italy.

Harrison, C. H. (**2003**). "Closed-form expressions for reverberation and signal-excess with mode-stripping and Lambert's law," J. Acoust. Soc. Am. **114**, 2744–2756.

Harrison, C. H. (**2005a**). "Closed form bistatic reverberation and target echoes with variable bathymetry and sound speed," IEEE J. Oceanic Eng. **30**, 660–675.

Harrison, C. H. (**2005b**). "Fast bistatic signal-to-reverberation-ratio calculation," J. Comput. Acoust. **13**, 317–340.

Harrison, C. H. (**2011a**). "Adiabatic reverberation and target echo mode incoherent sum: Artemis," NATO Undersea Res. Cent. Rep. NURC-FR-2011-009, NATO Undersea Research Centre, La Spezia, Italy, November 2011.

Harrison, C. H. (**2011b**). "The relation between the waveguide invariant, multipath impulse response, and ray cycles," J. Acoust. Soc. Am. **129**, 2863–2877.

Harrison, C. H. (**2012a**). "A relation between multipath group velocity, mode number, and ray cycle distance," J. Acoust. Soc. Am. **132**, 48–55.

Harrison, C. H. (**2012b**). "Retrieving ray convergence in a flux-like formulation," Tech. Rep. CMRE-FR-2012-006, Center for Maritime Research and Experimentation, Centre for Maritime Research and Experimentations, La Spezia, Italy, October 2012.

Harrison, C. H., and Ainslie, M. A. (**2010**). "Fixed time versus fixed range reverberation calculation: Analytical solution," J. Acoust. Soc. Am. **128**, 28–38.

Harrison, C. H., and Nielsen, P. L. (**2007**). "Multipath pulse shape in shallow water: Theory and simulation," J. Acoust. Soc. Am. **121**, 1362–1373.

Haskell, N. A. (**1951**). "Asymptotic approximation for the normal modes in sound channel wave propagation," J. Appl. Phys. **22**, 157–168.

Jensen, F. B., Kuperman, W. A., Porter, M. B., and Schmidt, H. (**1994**). *Computational Ocean Acoustics* (AIP, New York), pp. 155–185.

Morse, P. M., and Feshbach, H. (**1953**). *Methods of Theoretical Physics* (McGraw-Hill, New York), pp. 1092–1100.

Tolstoy, I., and Clay, C. S. (**1987**). *Ocean Acoustics: Theory and Experiment in Underwater Sound* (AIP, New York), pp. 145–150.

Urick, R. J. (**1967**). *Principles of Underwater Sound* (McGraw-Hill, New York), pp. 151–152.

Weston, D. E. (**1959**). "Guided propagation in a slowly varying medium," Proc. Phys. Soc. Lond. **73**, 365–384.

Weston, D. E. (**1960**). "A Moiré fringe analog of sound propagation in shallow water," J. Acoust. Soc. Am. **32**, 647–654.

Weston, D. E. (**1980a**). "Acoustic flux formulas for range-dependent ocean ducts," J. Acoust. Soc. Am. **68**, 269–281.

Weston, D. E. (**1980b**). "Acoustic flux methods for oceanic guided waves," J. Acoust. Soc. Am. **68**, 287–296.

Weston, D. E. (**1980c**). "Wave-theory peaks in range-averaged channels of uniform sound velocity," J. Acoust. Soc. Am. **68**, 282–286.

Westwood, E. K., Tindle, C. T., Chapman, N. R. (**1996**). "A normal mode model for acousto-elastic ocean environments," J. Acoust. Soc. Am. **100**, 3631–3645.

Zhou, J. X. (**1980**). "The analytical method of angular power spectrum, range and depth structure of echo-reverberation ratio in shallow water sound field," Acta Acust. **5**, 86–99 (in Chinese).

Document Data Sheet

Security Classification		Project No.

Document Serial No.	Date of Issue	Total Pages
CMRE-PR-2014-004	January 2014	13 pp.

Author(s)

Harrison, C.H.

Title

Ray convergence in a flux-like propagation formulation.

Abstract

The energy flux formulation of waveguide propagation is closely related to the incoherent mode sum, and its simplicity has led to development of efficient computational algorithms for reverberation and target echo strength, but it lacks the effects of convergence or modal interference. By starting with the coherent mode sum and rejecting the most rapid interference but retaining beats on a scale of a ray cycle distance it is shown that convergence can be included in a hybrid formulation requiring minimal extra computation. Three solutions are offered by evaluating the modal intensity cross terms using Taylor expansions. In the most efficient approach the double summation of the cross terms is reduced to a single numerical sum by solving the other summation analytically. The other two solutions are a local range average and a local depth average. Favourable comparisons are made between these three solutions and the wave model Orca with, and without, spatial averaging in an upward refracting duct. As a by-product, it is shown that the running range average is very close to the mode solution excluding its fringes, given a relation between averaging window size and effective number of modes which, in turn, is related to the waveguide invariant.

Keywords

Issuing Organization

Science and Technology Organization
Centre for Maritime Research and Experimentation

Viale San Bartolomeo 400, 19126 La Spezia, Italy

[From N. America:
STO CMRE
Unit 31318, Box 19, APO AE 09613-1318]

Tel: +39 0187 527 361
Fax:+39 0187 527 700

E-mail: library@cmre.nato.int